Magnetic phase diagram of Ho–Ag

2008 J. Phys.: Condens. Matter 20 104225

(http://iopscience.iop.org/0953-8984/20/10/104225)

J. Phys.: Condens. Matter **20** (2008) 104225 (5pp) doi:10.1088/0953-8984/20/10/104225

Magnetic phase diagram of Ho–Ag

V Paul-Boncour[1,5], A Hoser[2], K Hense[3], E Gratz[3], M Rotter[4] and N Stüßer[2]

[1] Chimie Métallurgique des Terres Rares, ICMPE, CNRS, 2 rue H Dunant, 94320 Thiais, France
[2] Hahn-Meitner Institut, Glienicker Strasse 100,14109, Berlin, Germany
[3] Institute for Experimental Physics, Technical University Vienna, Wiedner Hauptstrasse 8-10, A-1040, Austria
[4] Institut für Physikalische Chemie, Universität Wien, Währingerstrasse 42, 1090 Wien, Austria

E-mail: paulbon@glvt-cnrs.fr

Received 5 July 2007, in final form 18 September 2007
Published 19 February 2008
Online at stacks.iop.org/JPhysCM/20/104225

Abstract
The magnetic phase diagram of Ho–Ag has been established using magnetoresistance, magnetostriction and neutron diffraction experiments versus applied field and temperature. Three different magnetic phases were observed: an incommensurate antiferromagnetic phase (IC) below $T_N = 33$ K, a commensurate antiferromagnetic phase (C) above 5 T and below T_1 (5–8 K) and a ferromagnetic component above 3 T. The IC phase undergoes spin reorientations around 5 T (IC′) and 13 T (IC″).

1. Introduction

Rare earth (R) and silver form a series of intermetallic compounds RAg with CsCl type crystal structure. First studies of RAg compounds by susceptibility measurements showed an antiferromagnetic behaviour [1, 2]. Further works on RAg compounds indicated the existence of several antiferromagnetic phases depending on temperature and field [3–5].

In the case of HoAg its magnetic structure was solved by Nereson [12] using neutron diffraction without applied field. In the annealed magnetic state and below its Néel temperature $T_N = 33$ K, HoAg has an incommensurate antiferromagnetic structure with a sinusoidal modulated transverse spin wave propagating in the tetragonal ⟨100⟩ direction. The modulation wavelength is 6.6 ± 0.3 unit cell or 4.8 ± 0.2 nm. The Ho moments are oriented along the c axis with a maximal value of 8 μ_B. However, Kaneko *et al* [7] have performed high static magnetic field measurements and they have identified five magnetic transitions in HoAg for applied field up to 30 T. At 4.2 K the transition fields were located at $H_{c1} = 5.1$ T, $H_{c2} = 7.2$ T, $H_{c3} = 12.5$ T, $H_{c4} = 15$ T and $H_{c5} = 18$ T. At 27 T the saturation magnetization reaches 7.6 μ_B, close to the value determined by neutron diffraction. The temperature dependence of the critical field shows that H_{c1} decreases progressively, reaching zero at 30 K. H_{c2}, H_{c3}, H_{c4} and H_{c5} smeared out with increasing temperature and their temperature dependence could not be determined.

In order to clarify the HoAg magnetic phase diagram we have performed magnetoresistance, thermal expansion, magnetostriction and neutron diffraction experiments versus applied field and temperature. The analysis of magnetoresistance and magnetostriction measurements allowed us to determine the boundaries of the magnetic phase diagram, and the neutron diffraction to determine the magnetic structure of the different phases and their evolution versus field and temperature.

2. Experimental details

The HoAg compound was prepared by melting the pure elements in an induction furnace, ground up and annealed in vacuum at 600 K for 12 h. The compound was found to be single phase and crystallizes in a cubic structure with $a = 0.359\,72(2)$ nm.

The magnetoresistance and magnetostriction measurements were performed in the Vienna laboratories using standard methods in superconducting cryomagnets. For the magnetostriction a miniature capacitance dilatometer [8] was used with a polycrystalline sample of half cylindrical shape; the sample length was 1.85 mm. The field was applied parallel to the measurement direction.

[5] Author to whom any correspondence should be addressed.

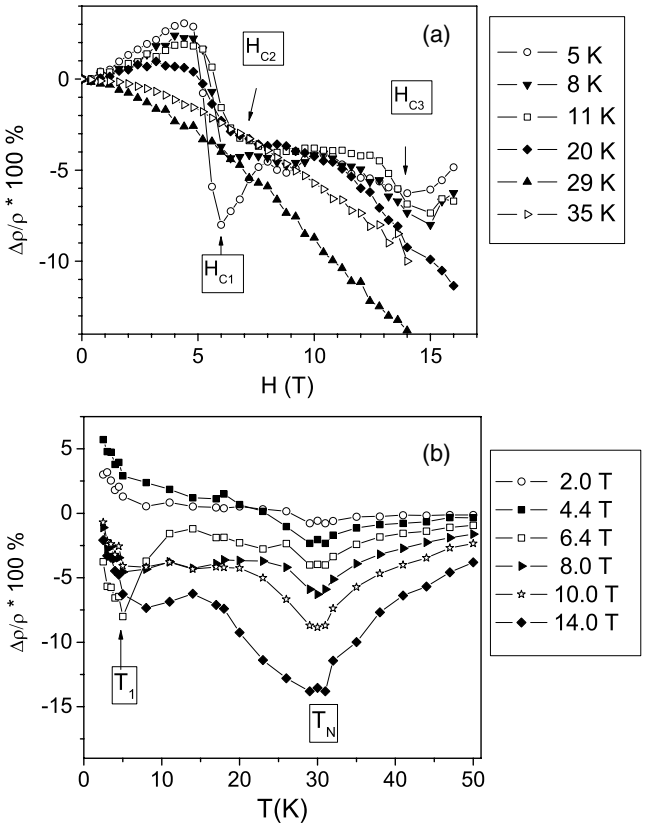

Figure 1. Evolution of the relative resistivity: (a) versus applied field at different temperatures and (b) versus temperature at different applied fields.

The neutron powder diffraction experiments were performed using the E1 and E6 instruments at BENSC in Berlin. The wavelengths were 0.2413 and 0.2454 nm for E1 and E6, respectively. The powder HoAg sample was frozen using deuterated alcohol to avoid preferred orientation of grains with the magnetic field. Due to geometrical limits of the 14 T magnet on one side and absorbing silver on the other side we used only 0.32 cm^3 sample volume in the neutron beam. For the same geometrical reasons we could not avoid strong peaks related to aluminium shielding.

The neutron diffraction patterns were refined using the Fullprof program [9].

3. Results

3.1. Magnetoresistance

In figure 1 are reported selected relative resistivity curves of HoAg versus applied field and temperature. The observed minima can be related to the transition fields and temperatures. From the curve analysis it is possible to identify the transition fields H_{c1} (5.5 T), H_{c2} (7.2 T) and H_{c3} (between 12 and 14 T). Similarly, transition temperatures are observed at T_1 (between 5 and 8 K) and T_N at 30 K, which is close to the Néel temperature of HoAg (33 K). The border lines of the HoAg magnetic phase diagram can be determined using these measurements. But as neutron diffraction is necessary to identify the magnetic structures of these phases in these different ranges, the complete phase diagram will be presented later in the discussion.

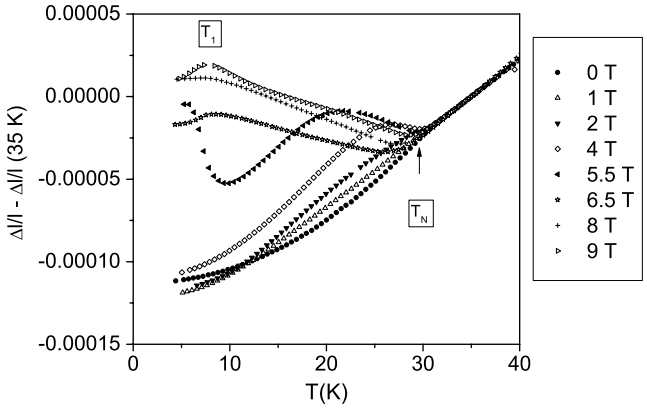

Figure 2. Thermal expansion of HoAg for different applied fields.

3.2. Thermal expansion and magnetostriction

The thermal expansion of HoAg has been measured at various applied fields between 0 and 9 T (figure 2). The curve anomalies are also used to determine the transition temperatures and fields. Here also two critical temperatures are observed, one around 8 K (T_1) for fields larger than 5 T and a second one at 30 K (T_N). The curve at $H = 5.5$ T displays a distinct shape marking clearly different thermal expansion behaviour below and above this critical field. Above the Néel temperature (33 K) all the curves display the same thermal expansion behaviour, which indicates a paramagnetic range. The small parastriction signal above 33 K and the pronounced features at the Néel temperature T_N indicate that the antiferromagnetic components are driving the magnetostriction in HoAg, possibly via the exchange striction mechanism [10]. The zero field thermal expansion is smooth and corresponds to a small spontaneous volume magnetostriction. The anisotropic strain may be larger but compensated due to the formation of antiferromagnetic domains or a possible multi-q structure in zero field. The change of sign of the thermal expansion which becomes negative between T_1 and T_N and fields between 6.5 and 9 T is probably related to a structural change which should be clarified by neutron diffraction.

3.3. Neutron diffraction

The NPD pattern of HoAg at $H = 0$ T and 2 K can be well refined with the modulated antiferromagnetic structure which was determined by Nerison [6] with a propagation vector (0.572, 0.5, 0) and a Ho moment of 8 μ_B. The magnetic line intensities progressively decrease as the temperature increases until the paramagnetic state is reached above the Néel temperature at 33 K.

As the applied field increases significant changes of the NPD patterns at 2 K are observed as shown on figure 3(a) for measurements on E1. Similar results were also observed at

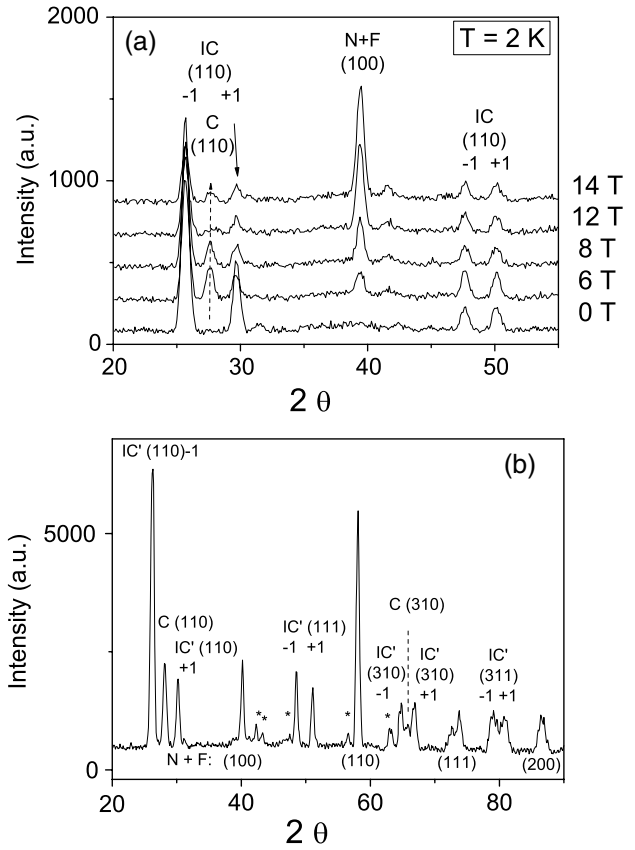

Figure 3. (a) Evolution of the NPD patterns of HoAg measured on E1 at 2 K for selected fields up to 14 T; (b) NPD pattern at 2 K and 6.5 T measured on E6 showing the coexistence of the three magnetic phases: incommensurate (IC′) and commensurate (C) antiferromagnetic phases and a ferromagnetic (F) component. ∗ sample holder contribution. The line indexations are in the (2a, 2a, a) supercell for the two antiferromagnetic phases and the (a, a, a) cell for the nuclear and ferromagnetic (N + F) lines.

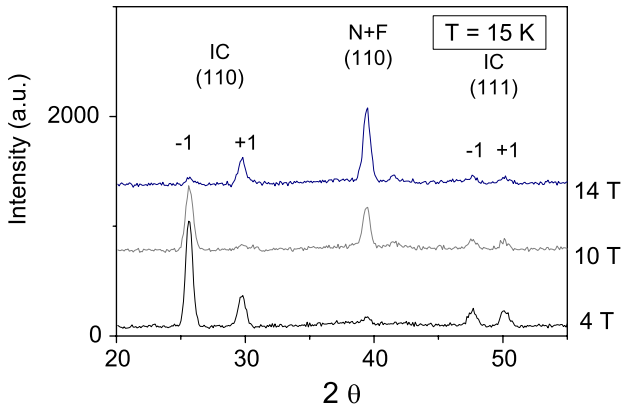

Figure 4. Evolution of selected NPD patterns at 15 K and different applied fields.

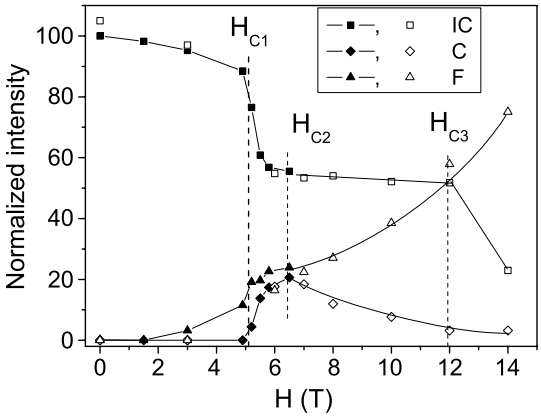

Figure 5. Normalized integrated line intensities at 2 K versus applied field (see the text). The dashed lines are guides for the eyes to indicate the transition fields.

5 K. At $H \geqslant 3$ T, the intensities of the nuclear lines start to grow, indicating the formation of a ferromagnetic component (F). This ferromagnetic component, which is also visible in the paramagnetic range, should be related to the formation of small ferromagnetic domains due to the application of the magnetic field. Above 5 T, the appearance of new lines which can be indexed with a (0.5, 0.5, 0) propagation vector corresponds to the formation of a commensurate antiferromagnetic phase (C). This magnetic structure has been already observed for GdAg [11] and DyAg below 9.5 K [4]. Above 5 T, a change of the satellite intensities of the (110), (310) and (311) reflexions belonging to the incommensurate phase, indicating a spin reorientation, is also observed. The relative intensities of the satellites of the (111) reflexions are not modified, showing that this reflexion is not affected by the spin reorientation. The full NPD pattern of HoAg at 6.5 T and 2 K measured on E6 (figure 3(b)) shows the coexistence of these three phases. The lines belonging to the incommensurate phase have been marked IC′ to take into account the spin reorientation.

The evolution of the NPD patterns at 15 K measured on E1 and displayed in figure 4 is representative of the region between 10 and 30 K. As the field increases the intensity of the IC phase line decreases and the intensities of the ferromagnetic line progressively increase. The change of the relative satellite line intensities is also attributed to a spin reorientation in the incommensurate phase.

In figure 5 is reported the evolution of the normalized line intensities at 2 K versus applied field corresponding to the IC, C and F phases measured on E6 (full symbol) and E1 (open symbol) spectrometers. The integrated and normalized intensities correspond to characteristic lines of each magnetic phase. One sharp transition is observed between 5 and 6 T with the growth of the C and F phases at the expense of the IC phase. Then between 7 and 12 T the ferromagnetic component increases continuously at the expense of the C phase. Above 12 T there is again a change of the satellite line intensities of the IC phase. The critical fields at 5.2, 6.5 and 12 T are close to the H_{c1}, H_{c2} and H_{c3} values reported in [7].

Similar results are observed at 5 K whereas at 10 K the C phase disappears, indicating that its Néel temperature is between 5 and 10 K. It should correspond to the T_1 temperature observed in resistivity and thermal expansion experiments. This can be clearly observed in figure 6, which reports the variation of characteristic line intensities of the different phases versus temperature at 7 T. In addition, it is seen that the

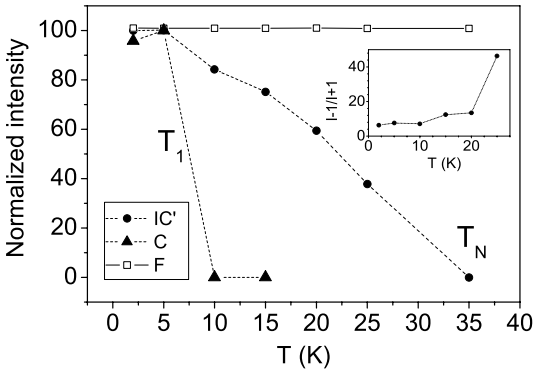

Figure 6. Evolution of the IC′, C and F normalized magnetic line intensities versus temperature at 7 T. The inset represents the evolution versus temperature of the ratio of the $-1/+1$ satellite intensity of the 110 line.

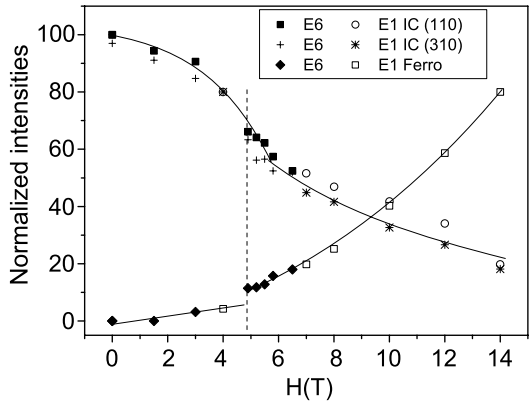

Figure 7. Normalized line intensities for IC and F phases at 15 K. The full symbol corresponds to E6 and the open symbol to E1 experiments.

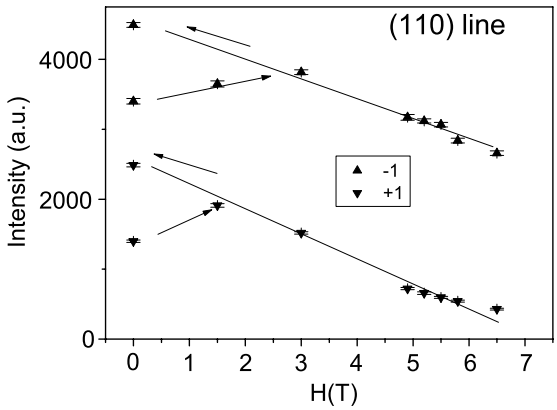

Figure 8. Line intensities of the two satellites of the (110) magnetic line. The arrows indicate the magnetic history of the sample, increasing the field from 0 to 6.5 T and reducing the field to 0 T.

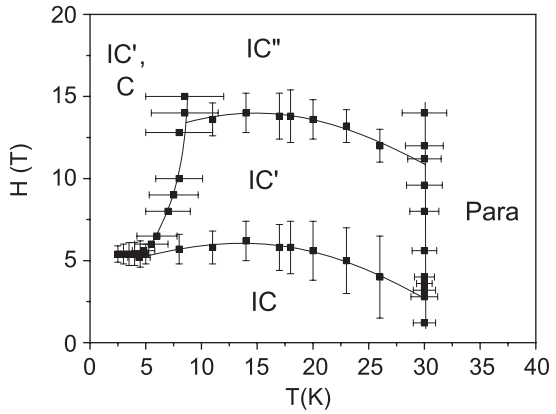

Figure 9. Ho–Ag magnetic phase diagram. IC represents the low temperature incommensurate phase with Ho moments parallel to the c axis; IC′ and IC″ indicate the incommensurate phase with the different spin reorientations. C represents the commensurate antiferromagnetic phase. The lines are guides for the eyes.

intensities of the IC phase lines decrease until 33 K, whereas the F component decreases only slightly versus T. In the inset is reported the evolution of the $-1/+1$ ratio of the (110) satellite line intensity. It increases slightly up to 20 K and sharply at 25 K, due to the strong decreases of the $+1$ satellite intensity. This change means that the angle between the Er spin and the c axis should increase with the temperature.

At 15 K a discontinuity is observed around 5 T, which corresponds to the critical field (H_{c1}) observed by magnetoresistance and magnetostriction measurements (figure 7). As the field increases above 5 T the position of the IC lines remains constant but some satellite line intensities are changing (figure 8): for the (110) reflection the -1 satellite increases at the expense of the $+1$ satellite; the two (111) satellites line intensities are not affected by the increase of the applied field whereas an increase of the -1 and $+1$ and a progressive disappearance of the -3 and $+3$ satellites of the (310) and (311) reflections is observed. In addition, as the field is decreased again to zero the system keeps the memory of this magnetic state (figure 8). This change of satellite line intensity can be attributed to a change of the spin orientation, with an angular deviation from the c axis as observed for ErAg [12]. At 14 T, a further change of the (110) satellite relative intensities is seen, indicating a second spin reorientation.

4. Discussion

The analysis of magnetoresistance and magnetostriction measurements established the phase diagram boundaries, whereas the neutron diffraction patterns reveal the structure of the phases and their evolution with field and temperature (figure 9). For low field below H_{c1} (5 T) and up to 30 K the main magnetic phase denoted IC corresponds to the modulated antiferromagnetic structure refined by Nerison [6] with a propagation vector of (0.572, 0.5, 0) and a Ho moment of 8 μ_B. Above 5 T and below T_1, the formation of the commensurate antiferromagnetic phase is observed. Between 6 and 12 T and below T_1, the ferromagnetic component grows at the expense of the commensurate one. The incommensurate phase is observed for all fields below $T_N = 33$ K. At $H = 0$, the Ho moments of the IC phase are oriented parallel to the c axis. However, the changes of the satellite line intensities above

5 T (IC′) and then 12 T (IC″) indicate two spin reorientations with angular deviation from the *c* axis. In addition, this spin reorientation is not fully reversible and is partially maintained if the field is decreased again to zero.

The ferromagnetic lines progressively increase with the applied field, but are not very sensitive to a change of temperature, for a given field. This continuous increase of the ferromagnetic component is in agreement with the evolution of the magnetization curve of HoAg at 4.2 K in [7], which increases almost continuously with field and reaches saturation only near 27 T. The transition fields H_{cn} appeared as small anomalies in the $M(H)$ curve. The ferromagnetic component is not reported in the phase diagram, since this contribution is observed even in the paramagnetic range and is due to a direct influence of the field and is not sensitive to the temperature. This means that this component is not related to the phase boundaries determined by magnetoresistance and magnetostriction experiments.

The magnetic behaviour of HoAg above 5 T presents some similarities with that of ErAg at $H = 0$ T [12]. In ErAg the C phase exists only at low temperature ($T_{NC} = 9.5$ K) and the Er moments are not parallel to the *c* axis, but present a tilt angle to the *c* axis of about 40°. In addition, in both compounds the change from a C to an IC phase at T_1 and close to the critical field H_{c1} is very abrupt and corresponds to a first order transition. This can be observed for HoAg in the thermal expansion behaviour at 5.5 T (figure 2) and in the variation of the normalized line intensity at 2 K and 7 T (figures 5 and 6). For field larger than 5.5 T the ferromagnetic component grows at the expense of the commensurate phase, and the thermal expansion is less affected by the disappearance of the commensurate phase. The negative slope of the thermal expansion between T_1 and T_N and for fields equal to or larger than 6.5 T should be attributed to the IC′ phase, when the Er spins are not oriented along the *c* axis. The decrease of the thermal expansion with the temperature is probably related to a change of the Er spin orientation versus temperature as observed in the NPD patterns at 7 T.

The transition at $T_N = 33$ K and 18 K for HoAg and ErAg respectively was attributed to the usual long range of the rare earth ions via the polarized conduction electrons [12].

In DyAg a change from C to IC is observed at 46.5 K, whereas the Néel temperature is at 56.6 K [13]. The Néel temperatures and the paramagnetic Curie temperatures were found to vary proportional to the Landé factor in the RAg intermetallic, when R is a heavy rare earth [1]. The complex magnetic phase diagram of DyAg versus field and temperature has been explained by an interplay between antiferromagnetic and antiquadrupolar interactions [14], which can also explain the HoAg behaviour.

5. Conclusion

The magnetic phase diagram of HoAg has been established using magnetoresistance, magnetostriction and neutron diffraction measurements. The incommensurate phase, with a 33 K Néel temperature, undergoes two spin reorientations around 5 and 12 T. The formation of a commensurate antiferromagnetic phase is observed above 5 T and below a temperature T_1 which increases from 5 to 8.5 K as the field increases. A ferromagnetic component, which starts to be visible at 3 T, increases with the applied field. The HoAg phase diagram has been compared with that of other RAg compounds and presents similarities with that of ErAg.

References

[1] Pierre J and Pauthenet R 1965 *C. R. Acad. Sci. Paris* **260** 2739
[2] Walline R E and Wallace W E 1964 *J. Chem. Phys.* **41** 3285
[3] Morin P and Schmitt D 1982 *J. Magn. Magn. Mater.* **28** 188
[4] Motokawa M, Arai M, Mino M, Ubukata K, Bokui T, Fujita M and Morin P 1995 *J. Magn. Magn. Mater.* **140–144** 1107
[5] Yoshii S, Kindo K, Nakanishi H and Kakeshita T 2004 *Physica* B **346/347** 160
[6] Nereson N 1972 *AIP Conf. Proc. N 5, Magnetism and Magnetic Materials* ed C D Graham and J J Rhyne (New York: American Institute of Physics) p 669
[7] Kaneko T, Abe S, Sakurada S, Yoshida H, Kido G and Nakagawa Y 1992 *J. Magn. Magn. Mater.* **104–107** 1401
[8] Rotter M, Müller H, Gratz E, Doerr M and Loewenhaupt M 1998 *Rev. Sci. Instrum.* **69** 2742
[9] Rodriguez-Carvajal J 1993 *Physica* B **192** 55
[10] Doerr M, Rotter M and Lindbaum A 2005 *Adv. Phys.* **54** 1
[11] Chattopadhyay T, McIntyre G J and Kobler U 1996 *Solid State Commun.* **100** 117
[12] Nereson N 1973 *J. Appl. Phys.* **44** 4727
[13] Kaneko T, Yoshida H, Ohashi M and Abe S 1987 *J. Magn. Magn. Mater.* **70** 277
[14] Morin P, Rouchy J, Yonenobu K, Yamagishi A and Date M 1989 *J. Magn. Magn. Mater.* **81** 247